



Contents lists available at ScienceDirect

Bioorganic & Medicinal Chemistry Letters

journal homepage: www.elsevier.com/locate/bmcl

Structure based evolution of a novel series of positive modulators of the AMPA receptor

Craig Jamieson^{a,*}, John K. F. Maclean^{a,*}, Christopher I. Brown^a, Robert A. Campbell^a, Kevin J. Gillen^a, Jonathan Gillespie^a, Bert Kazemier^b, Michael Kiczun^a, Yvonne Lamont^a, Amanda J. Lyons^a, Elizabeth M. Moir^a, John A. Morrow^a, John Pantling^a, Zoran Rankovic^a, Lynn Smith^a

^a Merck Research Laboratories, MSD, Newhouse, Motherwell, Lanarkshire ML1 5SH, UK

^b Merck Research Laboratories, MSD, PO Box 20, Oss, 5340 BH, Netherlands

ARTICLE INFO

Article history:

Received 1 October 2010

Revised 18 November 2010

Accepted 19 November 2010

Available online 25 November 2010

Keywords:

AMPA receptor

Allosteric modulator

SBDD

Indane

Scaffold hopping

ABSTRACT

Starting from compound **1**, we utilized biostructural data to successfully evolve an existing series into a new chemotype with a promising overall profile, exemplified by **19**.

© 2010 Elsevier Ltd. All rights reserved.

The α -amino-3-hydroxy-5-methyl-4-isoxazole-propionic acid (AMPA) receptors belong to the family of ionotropic glutamate ion channels. These receptor complexes are widely expressed in the central nervous system and are considered to mediate the majority of fast excitatory amino acid neurotransmission.¹ AMPA receptors appear to be crucial to facilitating synaptic plasticity and long-term potentiation (LTP), the use dependent enhancement in synaptic efficacy which is believed to underlie various forms of learning and memory. AMPA receptor modulators have been shown to enhance LTP and are, therefore, under serious consideration as therapeutic agents for a range of neurological disorders including schizophrenia, Alzheimer's Disease, Parkinson's disease and ADHD.^{2,3}

Our earlier work described the identification of **1** through optimization of an HTS-derived hit.^{4,5} Figure 1 depicts key properties of compound **1** alongside the X-ray co-crystal structure of **1** in complex with the GluA2 S1S2 Ligand Binding Domain (LBD) construct.⁶

In order to identify a new chemotype as a potential back-up series to that exemplified by **1**, we sought to leverage literature data

through exploiting our knowledge of the binding mode of our existing leads. The basic strategy adopted is delineated in Figure 2.

Compound **2**, a hydroxyl containing analogue of **1**, was considered to be a synthetically more expedient starting point and was shown to have similar potency⁷ and solubility (GluA1 pEC₅₀ = 6.4, solubility = 20 mg/L). We proposed to hybridize **2** with LY404187 (**3**), an AMPA receptor modulator which had previously been reported in the literature.⁸ In addition, the X-ray co-crystal structure of **3** was known,⁹ thus providing detailed knowledge of how the compound interacted with the receptor. Preparation and subsequent characterization of **4** indicated that the hybridized compound retained an acceptable balance of potency and solubility.

In vitro, compound **4** was shown to have excellent microsomal stability (rat Cl_i <12 μ L/min/mg protein, human Cl_i <12 μ L/min/mg protein) and reasonable permeability in a CaCo-2 assay, with no evidence of efflux (A–B = 206 nm/s, B–A = 287 nm/s). However, in vivo pharmacokinetic data was less promising (Cl_p = 49.7 mL/min/kg; T_{1/2} = 1.0 h; F% = 3.2; 1 mg/kg dose (iv), 5 mg/kg (po) using Wistar BRL rats). We hypothesized that the oral bioavailability of **4** could be improved by lowering clearance. Therefore, we considered conformational constraint of **4** with the expectation of being able to negate conformations predisposed to metabolism by CYP P450 enzymes. At the same time, we became aware of a related series of AMPA receptor modulators represented by **5** (Fig. 3)¹⁰ and thus sought to leverage those in our ligand constraint strategies.

Disappointingly, evaluation of **6** in the GluA2 functional assay indicated that the compound had only weak activity as an AMPA

* Corresponding authors at present address: Department of Pure and Applied Chemistry, University of Strathclyde, 295 Cathedral St, Glasgow G1 1XL, UK. Tel.: +44 1698 736496; fax: +44 1698 736187 (C.J.); tel.: +44 141 548 4830; fax: +44 141 548 5743 (J.K.F.M.).

E-mail addresses: craig.jamieson@strath.ac.uk (C. Jamieson), john.maclea@merck.com, john.maclea@btinternet.com (J.K.F. Maclean).

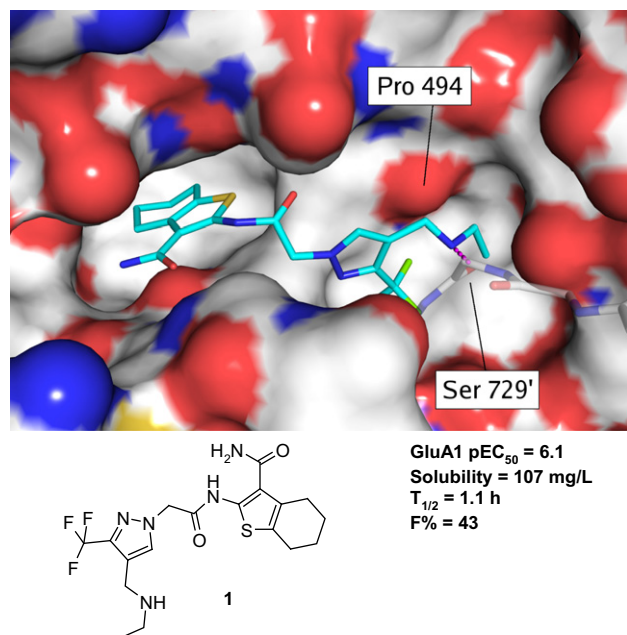


Figure 1. Lead compound **1**, summary property data and structure in complex with the GluA2 S1S2 LBD. As the binding site spans an intramolecular two-axis, two orientations of **1** are observed in the crystal structure, but only one is shown here. In this and subsequent figures,¹⁸ some residues are omitted for clarity, but main-chain atoms of residues 727–730 are here shown as sticks to illustrate the hydrogen bond between **1** and Ser 729'.

receptor modulator (pEC₅₀ <4.5). We then determined the X-ray structure of **4** in complex with the GluA2 S1S2 LBD,¹¹ which made it clear that the pyrazole moiety did not interact with the receptor in the same way as we anticipated from the structures of progen-

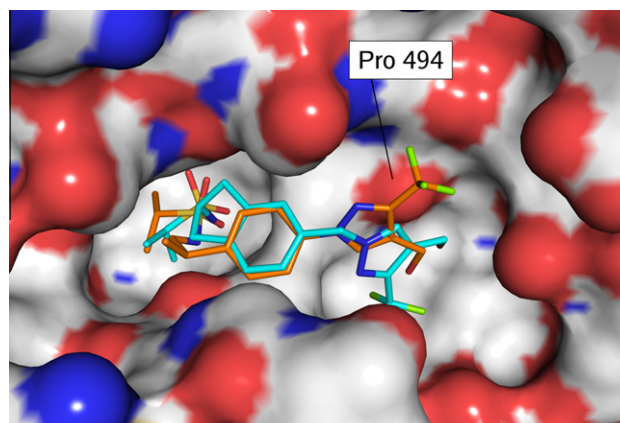


Figure 4. Overlaid X-ray structures of compounds **4** (carbons shown in orange) and **7** (carbons in cyan) in complex with the GluA2 S1S2 LBD. While the central phenyl rings overlay well, the orientations of the pyrazole fragments are very different. For **4**, the environment of the trifluoromethyl substituent is different to that observed for a related series [4,5], but the additional methylene in **7** allows the trifluoromethyl to return to the expected position.

itor compounds [4,5] such as **1** (Fig. 4). In particular, the pendant trifluoromethyl group, whose location in a hydrophobic pocket appeared a key binding element within other chemical series,^{12–14} was instead oriented away from the binding site. Modeling and conformational analysis suggested that insertion of a methylene spacer between the pyrazole group and central phenyl ring of **6** would be sufficient to alter the pyrazole orientation and restore this preferred interaction. Preparation and testing of compound **7** (GluA1 pEC₅₀ = 6.3) confirmed our hypothesis and the X-ray co-complex of **7** with the GluA2 S1S2 LBD (Fig. 4) demonstrated the binding mode was as anticipated from modeling.

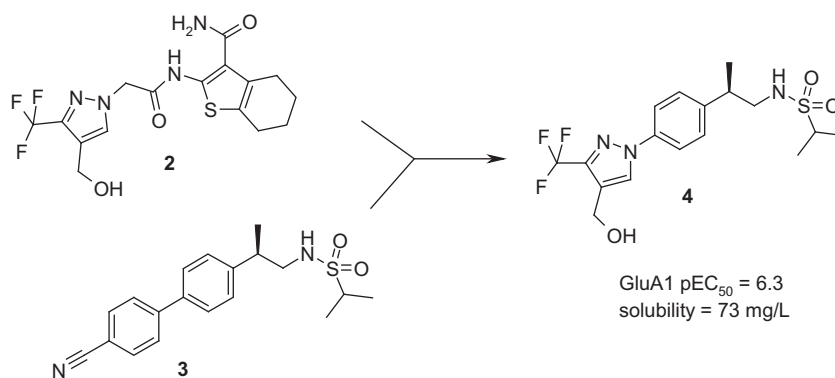


Figure 2. Lead series evolution through hybridization with literature compounds.

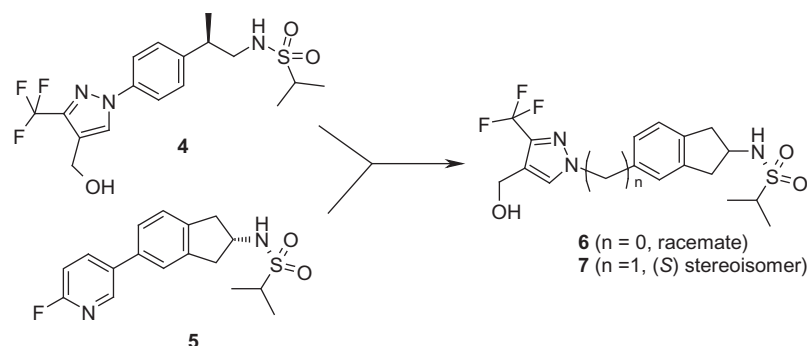


Figure 3. Introduction of conformational restraint.

It is intriguing that compound **4** retained potency in our GluA1 assay while **6** did not. Comparison of the co-crystal structures of **4** and **7** (Fig. 4) shows that the sulphonamide moiety is similarly positioned in each structure, but the central phenyl rings and attached pyrazoles adopt different orientations. Modeling suggests that the more constrained indane system is responsible for the drop in activity, as in contrast to **4**, molecule **6** does not have the conformational flexibility to correctly locate its sulphonamide while simultaneously positioning its pyrazole fragment in either of the preferred binding regions.

Compound **7** was shown to have good microsomal stability (rat Cl_i 31 μ L/min/mg protein, human Cl_i 23 μ L/min/mg protein) and reasonable permeability in a CaCo-2 assay, albeit with some

suggestion of efflux (A–B = 128 nm/s, B–A = 290 nm/s). Pleasingly, in vivo pharmacokinetic data was vastly superior when compared to compound **4**, with improved clearance and oral bioavailability (Cl_p = 21.6 mL/min/kg; T_{1/2} = 2.9 h; F% = 94; 1 mg/kg dose (iv), 5 mg/kg (po) using Wistar BRL rats).

Having suitably benchmarked compound **7**, our attention then turned to generation of a structure–activity relationship (SAR) within this constrained series. Our initial focus was in the pyrazole region which proved to be quite flexible in terms of which modifications were tolerated (Table 1).

Replacement (**8**) or homologation (**9**) of the pendant alcohol moiety had a minimal impact on potency. Similarly, the incorporation of fragments (compounds **10–12**) from our previously reported lead series [4,5] was reasonably well tolerated, with compound **10** gaining additional potency, albeit at the expense of solubility (<1 mg/L). The isomeric pyrazole system **13** was approximately 10-fold less potent, and this was attributed to the trifluoromethyl group being unable to make the same hydrophobic contact with the receptor as in compound **7**. The C-linked pyrazole system in compound **14** was also of similar potency compared to the progenitor compound as was the pyrrole based moiety **15**. Similarly, the furan derived system **16** demonstrated that diversification away from the original pyrazole motif could be achieved. Compound **16** was shown to bind to the receptor in a similar manner to **7**, the furan ring bioisosteric with the pyrazole ring and the trifluoromethyl group filling the hydrophobic pocket (Fig. 5).

Having explored the pyrazole region of **7**, we subsequently focused on the indane sulfonamide portion of the molecule (Table 2).

Comparing enantiomeric pairs such as compounds **7** and **17** and compounds **18** and **19** suggested that no distinct stereochemical preference existed within the series. Modification to the pendant isopropyl group was largely tolerated (**19–23**), although activity began to diminish when the size of the substituent was reduced (cf. **22** and **23**). Examination of the X-ray co-crystal structure of **7** points to the isopropyl group on the sulfonamide filling a hydrophobic pocket, which accounts for the trend observed. Substitution from the 1-position of the indanyl system resulted in an increase in potency (**24**) and related analogues (**25**, **26**) demonstrated a greater degree of flexibility in the SAR around sulfonamide substitution, with aryl sulfonamide derivatives also being tolerated (**27**, **28**).

Following additional profiling of a number of compounds in the series, compound **19** emerged as having the best overall balance of potency and developability properties. These are summarized in Table 3.

Compound **19** displayed high aqueous solubility and excellent stability in both microsomal and hepatocyte preparations. Permeability was predicted to be good from the CaCo-2 assay, with little evidence of efflux and this was mirrored in vivo with excellent oral

Table 1
Exploration of pyrazole region

Compds	R	pEC ₅₀ ^a
8		5.9
9		5.9
10		7.0
11		5.9
12		5.8
13		5.4
14		5.9
15		6.1
16		6.0

^a Values are means of two experiments performed in duplicate against GluA1.⁷

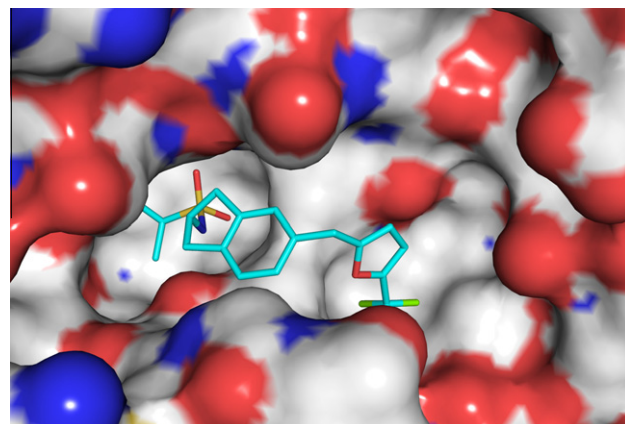
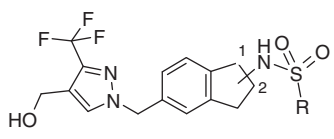
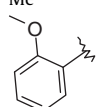
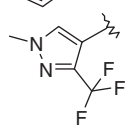


Figure 5. X-ray structure of compound **16** in complex with the S1S2J LBD of GluA2.

Table 2
SAR exploration of indane sulfonamide region

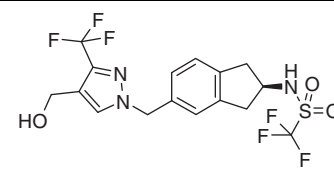


Compds	Position	Stereochem	R	pEC ₅₀ ^a
7	2	<i>S</i>	<i>i</i> Pr	6.3
17	2	<i>R</i>	<i>i</i> Pr	6.4
18	2	<i>S</i>	CF ₃	5.3
19	2	<i>R</i>	CF ₃	5.6
20	2	<i>R</i>	<i>c</i> Pr	5.6
21	2	<i>R</i>	NMe ₂	6.0
22	2	<i>S</i>	Et	6.4
23	2	<i>S</i>	Me	5.1
24	1	<i>rac</i>	<i>i</i> Pr	7.0
25	1	<i>rac</i>	<i>c</i> Pr	6.8
26	1	<i>rac</i>	Me	6.3
27	1	<i>rac</i>		5.7
28	1	<i>rac</i>		5.9

^a Values are means of two experiments performed in duplicate against GluA1.⁷

bioavailability observed, along with low clearance and highly encouraging half life. CNS exposure was determined through

Table 3
Developability properties of **19**



Property	
Solubility (mg L ⁻¹)	84
Microsomal stability (Clint, μg min ⁻¹ mg ⁻¹)	<12 (rat) <12 (human)
Hepatocyte stability (Clint, μl min ⁻¹ Mcells ⁻¹)	<6 (rat)
Caco2 (nm s ⁻¹)	169 (A–B) 264 (B–A)
Rat PK ^{a,b}	CL = 1.9 ml/(min/kg) V _{ss} = 1.0 L/kg T ^{1/2} = 7.4 h F% = 100
C _{max} Rat CSF ^c	0.12 μM

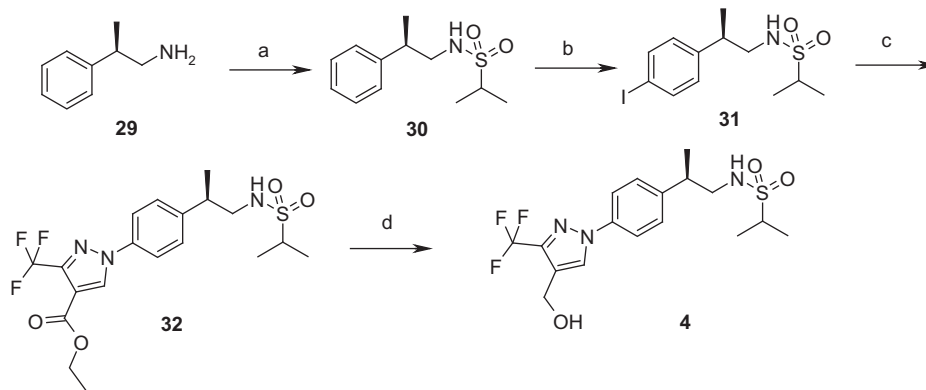
^a 2 mg/kg iv dose Wistar BRL rats.

^b 10 mg/kg po dose Wistar BRL rats.

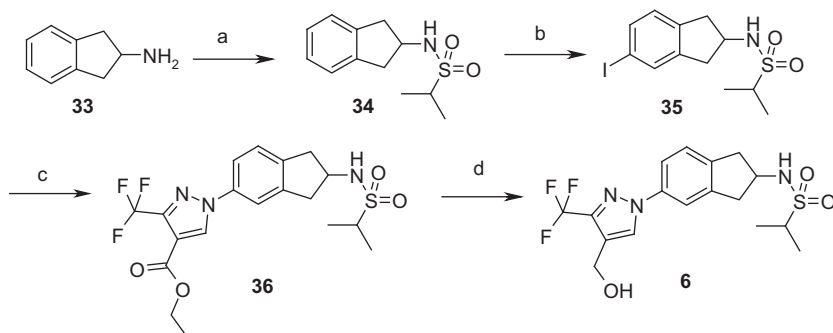
^c 2 mg/kg ip dose Wistar BRL rats.

measurement of drug concentration in CSF. This study showed good exposure and concentrations equivalent to the free drug in plasma, suggesting no efflux from the CNS.¹⁵

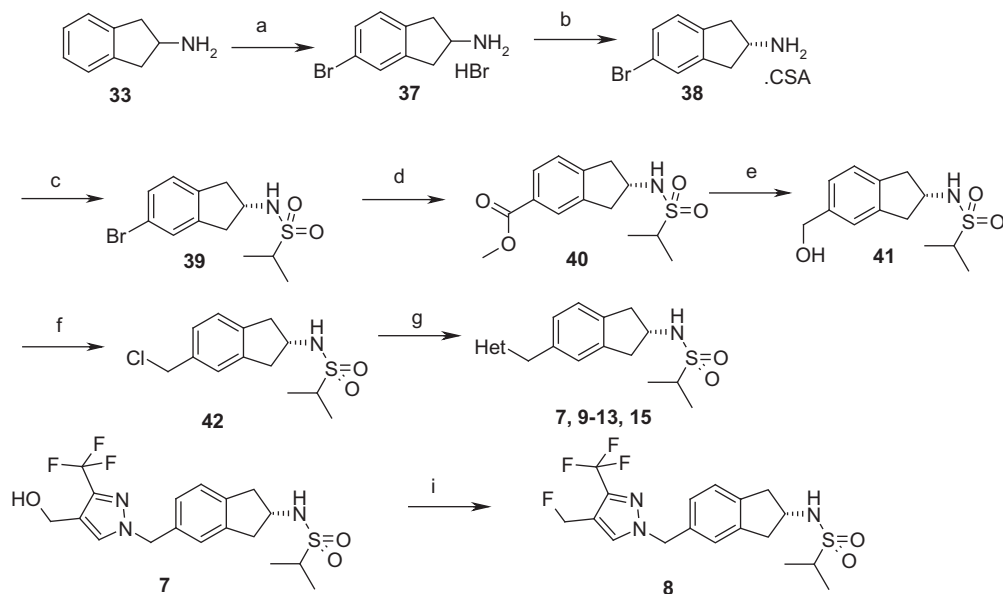
Synthesis of the compounds described above is outlined in Schemes 1–6. Sulfonylation of **29** (Scheme 1) followed by iodination and subsequent copper mediated arylation furnished **32**. Reduction with LiAlH₄ gave target compound **4**. Compound **6** was accessed in an analogous fashion as illustrated in Scheme 2.



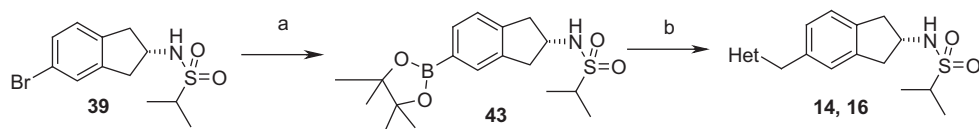
Scheme 1. Reagents and conditions: (a) *i*PrSO₂Cl, Et₃N, DMAP, CH₂Cl₂, rt, 87%; (b) I₂, H₂SO₄, AcOH, H₅IO₆, H₂O, 5 °C, 70%; (c) ethyl-3-(trifluoromethyl)pyrazole-4-carboxylate, CuI, *N,N*-dimethylcyclohexane-1,2-diamine, K₂CO₃, PhMe, 110 °C, 40%; (d) LiAlH₄, THF, rt, 52%.



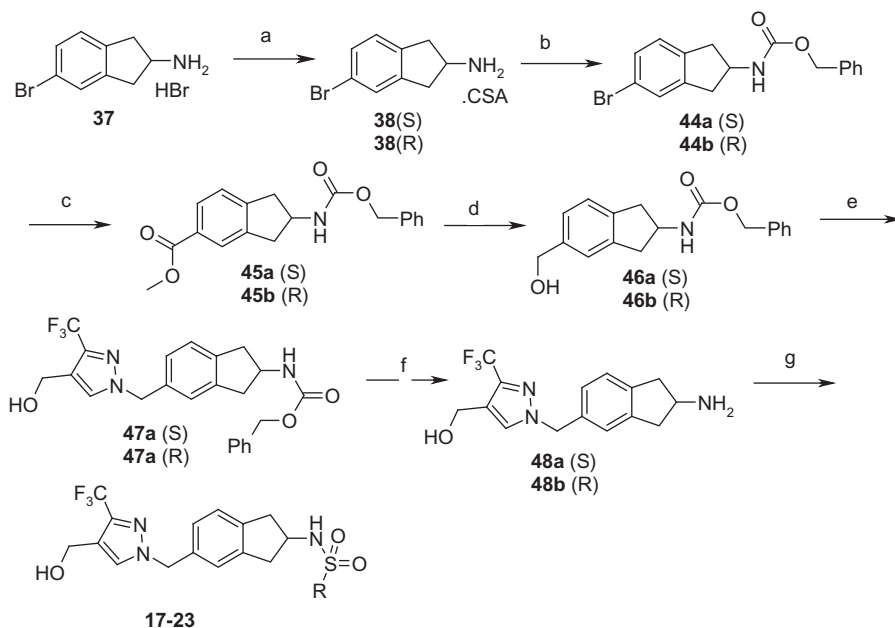
Scheme 2. Reagents and conditions: (a) *i*PrSO₂Cl, DBU, CH₂Cl₂, rt, 88%; (b) I₂, H₂SO₄, AcOH, H₅IO₆, H₂O, 5 °C, 56%; (c) ethyl-3-(trifluoromethyl)pyrazole-4-carboxylate, CuI, *N,N*-dimethylcyclohexane-1,2-diamine, K₂CO₃, PhMe, 110 °C, 16%; (d) LiAlH₄, THF, rt, 88%.



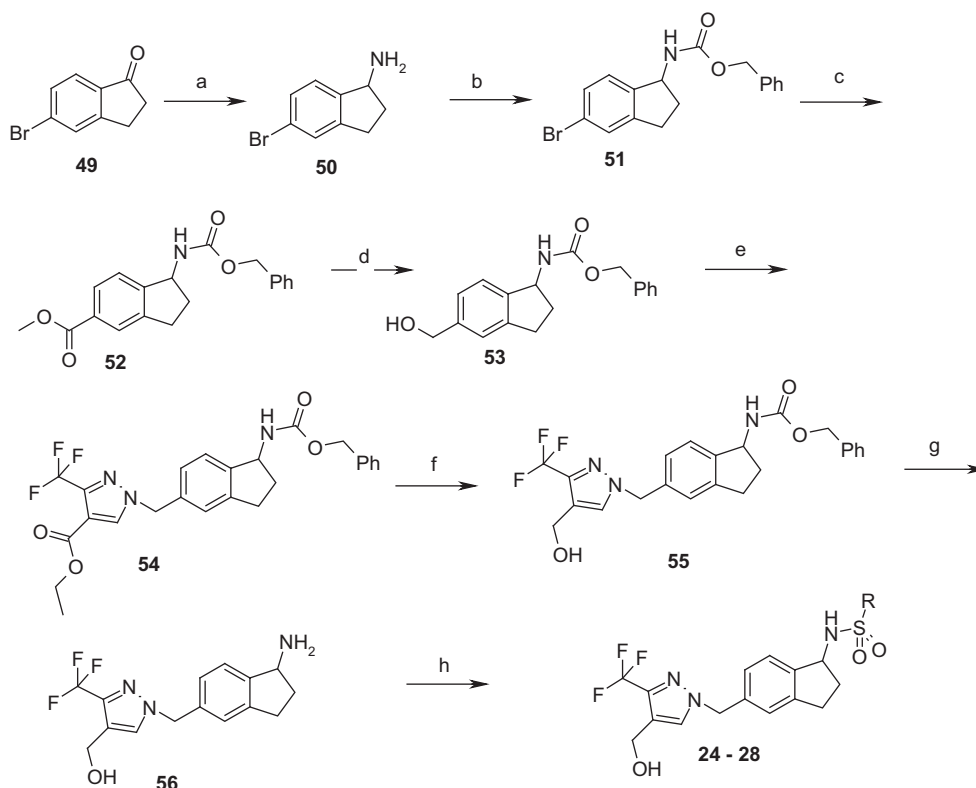
Scheme 3. Reagents and conditions: (a) Br_2 , H_2O , 60 °C, 56%; (b) L-camphorsulfonic acid, NMO, MeOH, 65 °C, 26%; (c) $i\text{PrSO}_2\text{Cl}$, DBU, CH_2Cl_2 , 0 °C, 93%; (d) acetoxy(2-(di-tolylphosphino)benzyl)palladium, $\text{P}^t\text{Bu}_3\text{-HBF}_4$, DBU, MeCN/MeOH, 150 °C, μW , 88%; (e) LiAlH_4 , THF, 0 °C, 100%; (f) SOCl_2 , CH_2Cl_2 , rt, 100%; (g) azole derivative, NaH, DMF, 60 °C, 19–55%; (i) DAST, CH_2Cl_2 , 20%.



Scheme 4. Reagents and conditions: (a) bis(pincolato)diboron, $\text{Pd}(\text{dppf})\text{Cl}_2$, KOAc, DMF, 60 °C, 41%; (b) HetCH_2Cl , $\text{Pd}_2(\text{dba})_3\text{-CHCl}_3$ complex, PPh_3 , NBS, Na_2CO_3 , 100 °C, μW , 16–20%.



Scheme 5. Reagents and conditions: (a) D or L-camphorsulfonic acid, NMO, MeOH, 65 °C, 26–30%; (b) benzyl chloroformate, K_2CO_3 , EtOAc/water; 100%; (c) acetoxy(2-(di-tolylphosphino)benzyl)palladium, $\text{P}^t\text{Bu}_3\text{-HBF}_4$, DBU, MeCN/MeOH, 150 °C, μW , 89–93%; (d) LiBH_4 , THF, rt, 48–51%; (e) (i) SOCl_2 , CH_2Cl_2 , rt; (ii) (3-(trifluoromethyl)-1H-pyrazolyl-4-yl)methanol, K_2CO_3 , 60 °C, 77–81% (over two steps); (f) $\text{Pd}(\text{OH})_2$, EtOH/5 N HCl, H_2 (2 bar), 66–71%; (g) sulfonyl chloride derivative or $(\text{CF}_3\text{SO}_2)_2\text{O}$ (for 18 and 19), Et_3N , CH_2Cl_2 , 17–71%.



Scheme 6. Reagents and conditions: (a) (i) $\text{NH}_2\text{OH}\cdot\text{HCl}$, EtOH, reflux; (ii) Zn , AcOH, rt 68% (over two steps); (b) benzyl chloroformate, K_2CO_3 , EtOAc/water; 67%; (c) acetoxymethyl-(2-(di-*o*-tolylphosphino)benzyl)palladium, $\text{P}^t\text{Bu}_3\text{HBF}_4$, DBU, MeCN/MeOH, 150 °C, μW , 77%; (d) LiAlH_4 , THF, rt, 48%; (e) (i) SOCl_2 , CH_2Cl_2 , rt; (ii) ethyl 3-(trifluoromethyl)-1*H*-pyrazol-4-ylcarboxylate, K_2CO_3 , 60 °C, 84% (over two steps); (f) LiAlH_4 , THF, rt, 74%; (g) $\text{Pd}(\text{OH})_2$, EtOH/5 N HCl, H_2 (2 bar), 83%; (h) sulfonyl chloride RSO_2Cl , Et_3N , CH_2Cl_2 , 24–32%.

Compounds **7**–**11** were prepared as outlined in Scheme 3. Bromination of 2-aminoindane followed by resolution¹⁶ gave enantiomerically pure amine **38**.

Sulfonylation followed by palladium mediated carbonylation and reduction gave alcohol **41** which could then be chlorinated and used to alkylate the appropriate azole derivative. Compound **8** was obtained directly from **7** by treatment with DAST, while compound **13** could be obtained via careful chromatographic separation from **7**.

Scheme 4 outlines the preparation of analogues **14** and **16**. The boronate ester **43** was prepared and used in a palladium catalysed $\text{sp}^2\text{--}\text{sp}^3$ coupling¹⁷ to furnish both target compounds.

Sulfonamide derivatives **17**–**23** were prepared according to the synthetic plan delineated in Scheme 5. Resolution of aminoindane **37** with either L- or D-CSA gave (*S*) or (*R*) enantiomers, respectively. Cbz protection followed by carbonylation and subsequent reduction gave **46a/46b** as separate compounds, both of which could be converted to the chloride derivative and used to alkylate the requisite pyrazole alcohol. Protecting group removal followed by the final diversity step gave target compounds **17**–**23** as discrete enantiomers.

Compounds **24**–**28** were prepared in an analogous fashion to the above starting from 5-bromo-2,3-dihydro-1*H*-inden-amine (**50**) which is prepared via reduction of an oxime intermediate derived from 5-bromoindan-1-one (**49**, Scheme 6).

In summary, a critical component of our scaffold hopping strategy has been the application of structure-based drug design (SBDD) against an ion channel target, both directing our template modifications and offering key insights into SAR within the series. Starting from lead compound **1**, we have demonstrated optimization to yield a structurally differentiated entity (**19**) with an excellent overall balance of properties. We believe **19** will be a

valuable tool in further understanding the potential role of AMPA receptor modulators in complex neurological disorders.

References and notes

- Kew, J. N. C.; Kemp, J. A. *Psychopharmacology* **2005**, 179, 4.
- Marenco, S.; Weinberger, D. R. *CNS Drugs* **2006**, 20, 173.
- Zarate, J.; Manji, H. K. *Exp. Neurol.* **2008**, 211, 7.
- Jamieson, C.; Basten, S.; Campbell, R. A.; Cumming, I. A.; Gillen, K. J.; Gillespie, J.; Kazemier, B.; Kiczun, M.; Lamont, Y.; Lyons, A. J.; Maclean, J. K. F.; Moir, E. M.; Morrow, J. A.; Papakosta, M.; Rankovic, Z.; Smith, L. *Bioorg. Med. Chem. Lett.* **2010**, 20, 5753.
- Jamieson, C.; Campbell, R. A.; Cumming, I. A.; Gillen, K. J.; Gillespie, J.; Kazemier, B.; Kiczun, M.; Lamont, Y.; Lyons, A. J.; Maclean, J. K. F.; Martin, F.; Moir, E. M.; Morrow, J. A.; Pantling, J.; Rankovic, Z.; Smith, L. *Bioorg. Med. Chem. Lett.* **2010**, 20, 6072.
- Armstrong, N.; Sun, Y.; Chen, G. Q.; Gouaux, E. *Nature* **1998**, 395, 913.
- HEK-GluR1(i) cells were maintained in DMEM supplemented with 10% fetal calf serum, 1% non-essential amino acids and 150 $\mu\text{g}/\text{mL}$ hygromycin, at 37 °C/5% CO_2 . Twenty-four hour prior to the assay, the cells were harvested with trypsin and seeded onto Costar 96-well clear bottomed black plates at a density of 3.5×10^4 per well. Cells were loaded with 5 μM fluo3-AM in DMEM media in the absence of hygromycin and incubated at 37 °C/5% CO_2 for 1 h. After dye loading, the cells were washed once with 200 μL of low calcium solution (10 mM HEPES, pH 7.4, 160 mM NaCl, 4.5 mM KCl, 2 mM CaCl_2 , 1 mM MgCl_2 , 10 mM glucose) containing 0.625 mM of probenecid to remove the dye. Then 200 μL of low calcium solution was added to each well. The FLEXstation added 50 μL of glutamate +/- test compound in high calcium solution (10 mM HEPES, pH 7.4, 160 mM NaCl, 4.5 mM KCl, 20 mM CaCl_2 , 1 mM MgCl_2 and 10 mM glucose) to each well and the ensuing response was monitored on FLEXstation.
- Quirk, J. C.; Nisenbaum, E. *CNS Drug Rev.* **2002**, 8, 255.
- Sobolevsky, A. I.; Rosconi, M. P.; Gouaux, E. *Nature* **2009**, 462, 745.
- Ward, S. E.; Harries, M.; Aldegheri, L.; Andreotti, D.; Ballantine, S.; Bax, B. D.; Harries, A. J.; Harker, A. J.; Lund, J.; Melarange, R.; Mingardi, A.; Mookherjee, C.; Mosley, J.; Neve, M.; Oliosi, B.; Profeta, R.; Smith, K. J.; Smith, P. W.; Spada, S.; Thewlis, K. M.; Yusuf, S. P. *J. Med. Chem.* **2010**, 53, 5801.
- Crystals were grown as described in Ref.⁴ Co-crystallizations were performed by soaking *apo* crystals in 100 mM test compound for 24 h prior to data collection. Coordinates and structure factors have been deposited with the

- Protein Data Bank for complexes of compounds **1** (3O6H), **4** (3PMV), **7** (3PMW), **16** (3PMX).
12. Grove, S. A. J.; Jamieson, C.; Maclean, J. K. F.; Morrow, J. A.; Rankovic, Z. *J. Med. Chem.* **2010**, *53*, 7271.
 13. Ward, S. E.; Harries, M. *Curr. Med. Chem.* **2010**, *17*, 3503.
 14. (a) Bradley, D. M.; Chan, W. N.; Harrison, S. A.; Thatcher, R.; Thewlis, K. A.; Ward, S. E. PCT Int. Appl. WO07107539, 2007. (b) Gillen, K.; Jamieson, C.; Maclean, J. K. F.; Moir, E. M.; Rankovic, Z. PCT Int. Appl. WO08003452, 2008. (c) Bradley, D. M.; Chan, W. N.; Harrison, S. A.; Thewlis, K. A.; Ward, S. E. PCT Int. Appl. WO08110566, 2008. (d) Bertheleme, N.; Bradley, D. M.; Cardullo, F.; Merlo, G.; Pozzan, A.; Scott, J. S.; Thewlis, K. A.; Ward, S. E. PCT Int. Appl. WO08113795, 2008. (e) Bradley, D. M.; Chan, W. N.; Ward, S. E. PCT Int. Appl. WO08148836, 2008.
 15. Lin, J. H. *Curr. Drug Metab.* **2008**, *9*, 46.
 16. Prashad, M.; Hu, B.; Har, D.; Repic, O.; Blacklock, T. J.; Acemoglu, M. *Adv. Synth. Catal.* **2001**, *343*, 461.
 17. Burns, M. J.; Fairlamb, I. J. S.; Kapdi, A. R.; Sehnal, P.; Taylor, R. J. K. *Org. Lett.* **2007**, *9*, 5397.
 18. [Figures 1, 4 and 5](#) were prepared using the PyMOL Molecular Graphics System, Schrödinger, LLC.